DOI: 10.17344/acsi.2019.5790 *Acta Chim. Slov.* **2020,** *67,* 830–841
creative commons

Scientific paper

Prediction of Biological Activities, Structural Investigation and Theoretical Studies of *meta*-cyanobenzyl Substituted Benzimidazolium Salts

Duygu Barut Celepci[1,*] and Aydın Aktaş[2,3]

[1] *Dokuz Eylül University, Faculty of Science, Department of Physics, İzmir, Turkey*

[2] *İnönü University, Vocational School of Health Service, 44280, Malatya, Turkey*

[3] *İnönü University, Faculty of Science, Department of Chemistry 44280, Malatya, Turkey*

* *Corresponding author: E-mail: duygu.barut@deu.edu.tr*

Received: 12-18-2019

Abstract

The structural properties of *meta*-cyanobenzyl substituted *N*-heterocyclic carbene (NHC) precursors were investigated theoretically. The molecular and crystal structure of one of the compounds was determined by using the single-crystal X-ray diffraction method. Global reactivity descriptors were analyzed to understand the biological activity behaviors of the compounds with *Density Functional Theory* (DFT) B3LYP method with 6-31G* basis set. Vibrational frequencies, chemical shifts and absorption wavelengths were computed and compared to experimental data. A predictive study for the biological activities was done using PASS (prediction of activity spectra for biologically active structures) online software. Biological activity predictions showed the analgesic, substance P antagonist, non-opoid and antiinflammatory activities of the compounds.

Keywords: *N*-heterocyclic precursors; crystal structure; DFT; PASS online

1. Introduction

N-heterocyclic carbenes (NHC) are cyclic carbenes containing at least one amino substituent.[1] NHCs were first pioneered by Öfele, Wanzlick, and Schönherr in 1968 and the isolation of the first stable crystalline carbene was performed by Arduengo in 1991.[2–4] After the stability of the NHC ligands was registered, they have been attracted great interest in the field of organic and organometallic chemistry. Especially, in medical applications, there have been various studies of metal-NHCs.[5–7] The chelating effect of NHC precursors with unique sigma donor properties could be effective in biological activity.[8,9] In our previous study, the investigations on the biological activity of NHC compounds containing cyanobenzyl substituents show that these compounds have exhibited biological activity.[10]

Biological experiments are often limited in terms of sample, time and cost. In this context, DFT-based reactivity descriptors are advantageous and generally be consistent with the experimental observations.[11] In recent years, the prediction of the reactivity of chemical systems is one of the main purposes of theoretical chemistry. Density functional theory (DFT) has been quite successful in providing the theoretical groundwork of this purpose. For analyzing and understanding the biological reactivity of the chemical systems, several reactivity descriptors have been proposed. In this work, biological reactivity studies of three compounds **2b**, **2f** and **2g** were carried out through these global reactivity descriptors. Geometries of the compounds were optimized and bonding parameters were compared to the experimental data. Frontier molecule orbitals (HOMO and LUMO) and the energy values were computed. Natural bond orbital (NBO) analysis was used to analyze the stability of the molecules arising from hyperconjugative interactions and charge delocalization. The vibrational frequencies, chemical shifts and absorption wavelengths were calculated and compared to the experimental ones. Also, PASS (prediction of activity spectra for biologically active structures) online software was used to predict the putative biological activity spectra of the compounds. DFT studies and PASS online predictions point out the similar activity results for the compounds.

It is believed that this kind of study will contribute to getting a better understanding of the chemical behavior of *meta*-cyanobenzyl substituted benzimidazolium salts. As proved by enzyme inhibition studies,[10] these compounds can be a candidate as new drugs for therapy of some diseases such as glaucoma, epilepsy, gastric and duodenal ulcers, osteoporosis, mountain sickness, or neurological disturbances.

2. Experimental

The synthesis, some spectroscopic results and enzyme inhibition studies of the compounds **2b**, **2f**, **2g** and single-crystal X-ray diffraction studies of the **2f** and **2g** were reported previously.[10] In this work, firstly, we determined the crystal structure of **2b** by single-crystal X-ray diffraction method. Then, the theoretical studies were performed for all structures.

2. 1. X-ray Crystallography

The single-crystal X-ray diffraction study of the compound **2b** was performed by ω-scan technique, using a Rigaku-Oxford Xcalibur diffractometer with an EOS-CCD area detector operated at 50 kV and 40 mA using graphite-monochromated MoKα radiation (λ = 0.71073 Å) from an enhance X-ray source with CrysAlis^{Pro} software.[12] Data reduction and analytical absorption corrections were carried out by CrysAlis^{Pro} program.[13] The structure was solved by the *Intrinsic Phasing* method with SHELXT and refined utilizing the SHELXL program[14,15] incorporated in the OLEX2 program package.[16] The crystallographic data and some parameters of refinement are placed in Table 1. Anisotropic thermal parameters were applied to all non-hydrogen atoms. All the hydrogen atoms were placed using standard geometric models and with their thermal parameters riding on those of their parent atoms.

2. 2. Computational Details

The compounds **2b**, **2f** and **2g** were optimized, chemical shifts and frontier molecular orbital energies were carried out by using DFT/B3LYP with the basis set 6-31G* by Gaussian 09W and GaussView 6.0 molecular visualization programs.[17,18] Natural bond orbital (NBO) analysis was performed using NBO 3.1 program as implemented in the Gaussian 09 package at the same level of the theory.[19] The normal mode assignments of the compounds were employed by VEDA[20] program and verified by GaussView 6.0. The NMR chemical shifts were computed in the gaseous state within GIAO (Gauge-Independent Atomic Orbital) approach by subtracting the shielding constants of TMS.[21] The biological activity spectra of studied compounds **2b**, **2f** and **2g** were obtained by the PASS Online Program (http://www.way2drug.com/PASSOnline/).

3. Results & Discussions

3. 1. Crystal Structure of Compound 2b

Single-crystal X-ray diffraction analyses reveal that the compound **2b** crystallizes in the orthorhombic space

Table 1. Crystal data and experimental details for the compound **2b**.

Empirical Formula	$C_{23}H_{20}BrN_3$
Formula Weight	418.33
Temperature (K)	293(2)
Crystal System, space group	Orthorhombic, *Pca2$_1$*
a, b, c (Å)	14.6406(7), 7.9998(4), 17.0884(9)
α, β, γ (°)	90, 90, 90
V (Å^3)	2001.43(17)
Z	4
Density (calculated) (g/cm^3)	1.388
Absorbtion coefficient (μ, mm^{-1})	2.066
F(000)	856
Crystal size (mm^3)	0.360 × 0.259 × 0.253
Radiation	MoKα (λ = 0.71073)
2θ range for data collection (°)	6.054 to 51.364
Index ranges	$-10 \leq h \leq 17$, $-9 \leq k \leq 9$, $-20 \leq l \leq 20$
Reflections collected	8295
Independent reflections	3441 [R_{int} = 0.0322, R_{sigma} = 0.0441]
Restraints/Parameters	4/245
Goodness-of-fit on F^2	1.015
Final *R* indices [$I \geq 2\sigma(I)$]	R_1 = 0.0335, wR_2 = 0.0599
R indices	R_1 = 0.0529, wR_2 = 0.0661
Largest diff. peak/hole (eÅ^{-3})	0.20/–0.20

group $Pca2_1$. The asymmetric unit of the compound contains a *meta*-cyanobenzyl-substituted benzimidazolium cation and a bromide anion (Fig. 1). The single-crystal X-ray diffraction studies reveal that the benzimidazolium ring system is almost coplanar with the r.m.s. deviation of 0.007(6) Å. Cyanobenzyl and methylbenzyl fragments lie to the different sides of the benzimidazole ring system, giving the cation a Z-shape. The dihedral angles between the benzimidazolium ring and the mean plane of these fragments are 67.83(9)° and 69.27(2)°, respectively. Two C–H···Br type intermolecular interactions are observed in the crystal structure; one is between the most acidic proton of the imidazolium cation and the bromide anion [C1–H1···Br1, H1···Br1 = 2.61 Å, C1–Br1 = 3.545(5) Å, C1–H1···Br1=155°], the other interaction is C16–H16B···$Br1^i$ [H16B···$Br1^i$ = 2.85 Å, C16–$Br1^i$ = 3.813(6) Å, C1–H1···$Br1^i$ = 170°]. Fig.2 displays the infinite chain occurs *via* these hydrogen bonds along the *b*-axis. The molecules stacked in the crystal structure to form a *pincers-like* packing motif, as shown in Fig. 3.

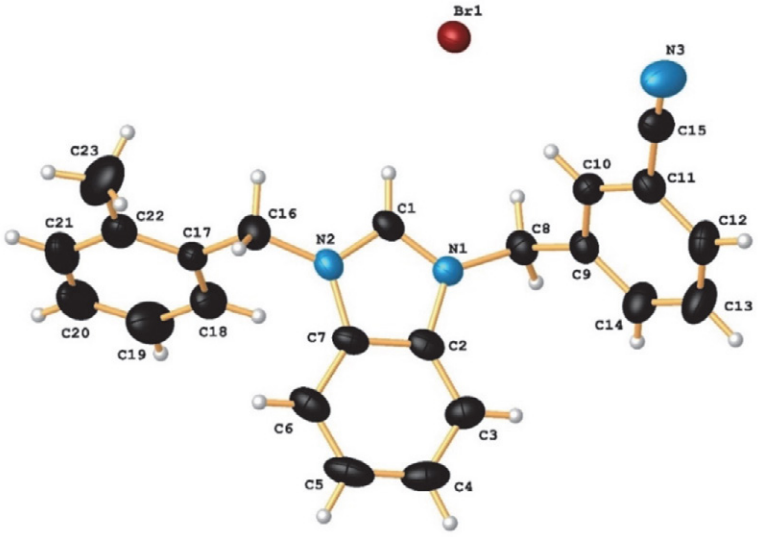

Fig. 1. Structure of **2b** with ellipsoids plotted at 30% probability. Selected bond parameters (Å,°): N1–C1 1.327(6), N1–C2 1.389(5), N1–C8 1.472(5), N2–C1 1.326(5), N2–C7 1.389(6), N2–C16 1.459(6), N3–C15 1.138(7); N1–C1–N2 111.0(4), C1–N1–C8 125.6(4), N1–C8–C9 113.2(4), C2–N1–C8 126.3(4), C1–N2–C16 125.4(4), C7–N2–C16 127.0(4), N2–C16–C17 113.0(4), C11–C15–N3 177.2(8).

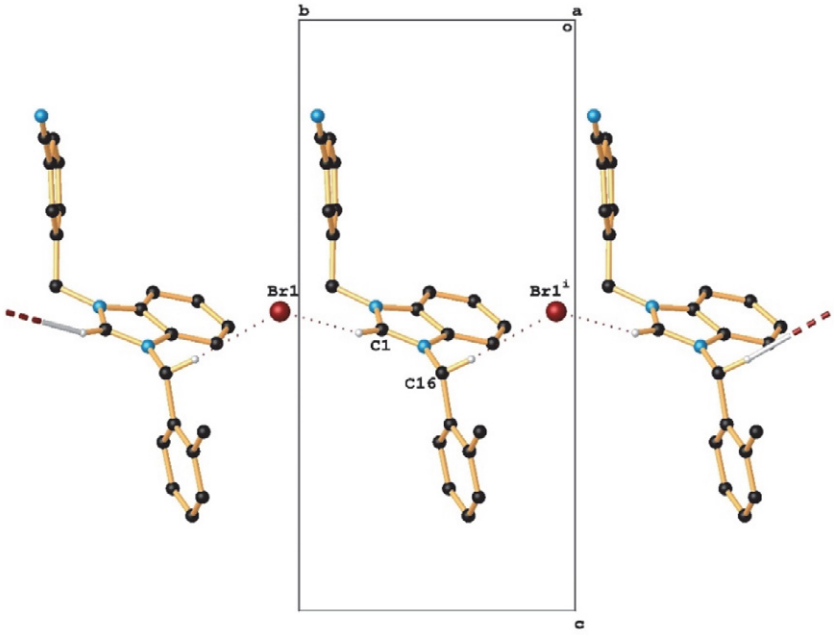

Fig. 2. Packing of the cation molecules of **2b** through the intermolecular hydrogen bonds bridged by the bromide anions, which lead to the infinite chain along the *b* axes. All hydrogen atoms except those participating in the hydrogen bonds were omitted for clarity. Cation molecules are shown in the stick drawing style.

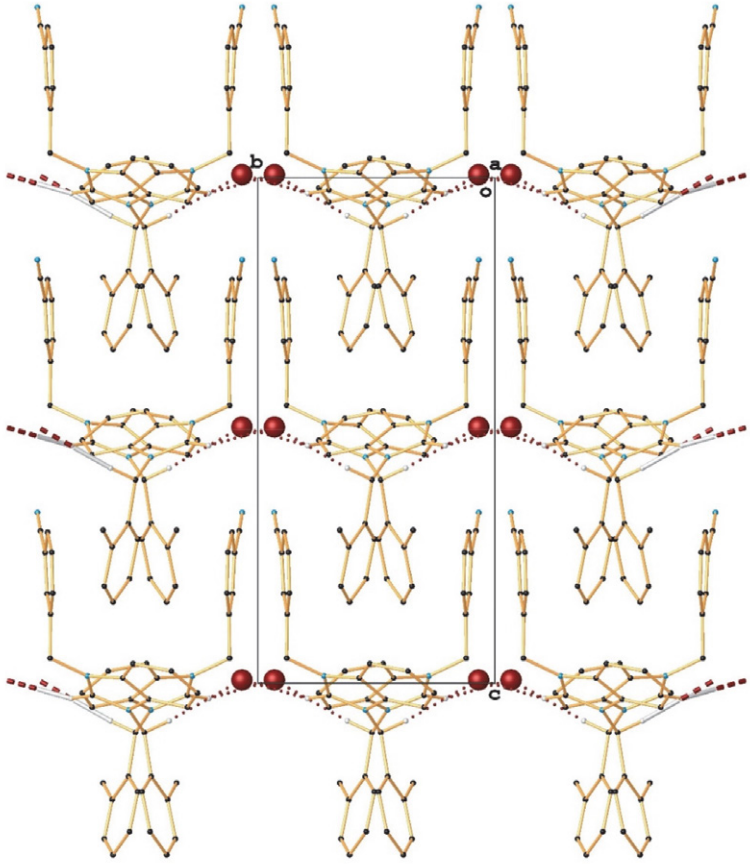

Fig. 3. Graphical representation of *pincers-like* packing motif the molecules within the unit cell for **2b.**

3. 2. Geometry Optimization, Frontier Molecular Orbitals and Global Reactivity Descriptors

The optimized ground state geometry of the compounds at DFT/B3LYP/6-31G* level of the theory is shown in Fig. 4. The correlations between the theoretical and experimental bonding parameters were displayed in Fig. S1 (see supplementary information file). It is clearly understood from the figure that there are some discrepancies between the experimental and computed bond parameters. While the theoretical calculations of the isolated structure were carried out in the gas phase, the fact that the experimental molecular structures were in a solid-state form likely caused these differences. Also, the experimental structures have intermolecular interactions, which may cause discrepancies in the bonding parameters.

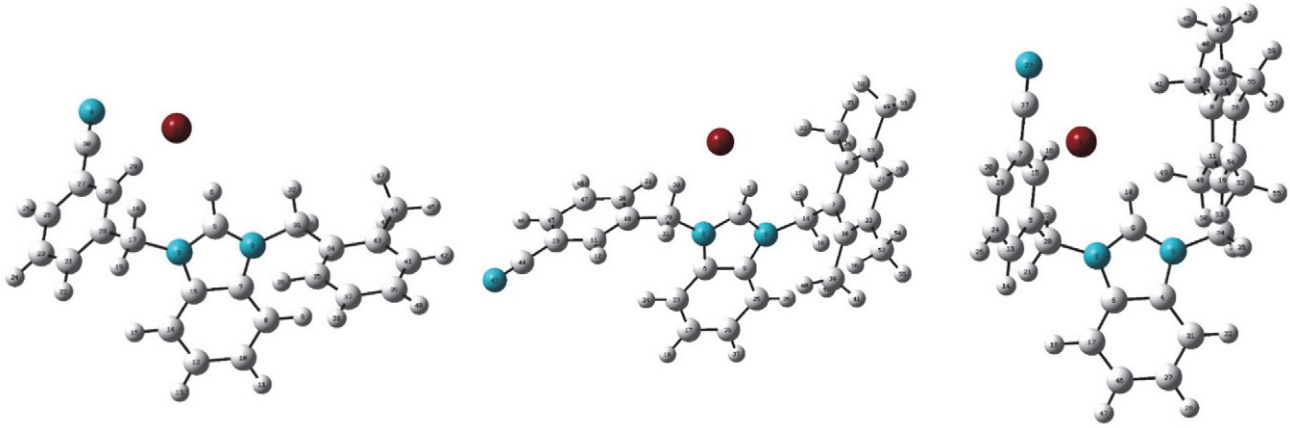

Fig. 4. Optimized geometries of the compounds **2b**, **2f** and **2g**, respectively.

The FMOs theory involving HOMO and LUMO is one of the best theories to get an insight into the chemical stability of a molecule.[22] The highest occupied molecular orbital (HOMO) represents the distribution and energy of the least tightly held electrons in the molecule and the lowest unoccupied molecular orbital (LUMO) describes the easiest route to the addition of more electrons to the system. The high value of E_{HOMO} indicates the ease of donating an electron to the unoccupied orbital of the receptor molecule, and the small value of E_{LUMO} means that it has small resistance to accept electrons so it will be more able to accept electrons. The difference between HOMO and LUMO energy values gives the HOMO-LUMO energy gap (E_{gap}) and it is an important stability index.[23] A molecule with large E_{gap} is described as a hard molecule, much less polarizable, and implies high molecular stability and aromaticity low reactivity in chemical reactions.[24,25] The soft systems have small E_{gap}, they are highly polarizable and exhibit a significant degree of intramolecular charge transfer from the electron donor to the electron acceptor and conjugation that may influence the biological activity of the molecule.[26]

To evaluate the energetic behavior of the compounds, the HOMO-LUMO analysis was carried out by using B3LYP/6-31G* method, and the plots are depicted in Table 2. As can be seen, compounds show different localization of the HOMOs and LUMOs. The HOMO of the **2b** and **2g** is located on the bromide anions, while in **2f**, it is distributed to the bromide anion and the benzimidazolium fragment of the cation molecule. Similarly, LUMO electron density of **2f** is spread over the cyanobenzyl moiety, but for **2b** and **2g**, the LUMO electrons are mainly located on the benzimidazolium ring. The values of energy separation between the HOMO-LUMO were found as 2.930, 3.845 and 3.011 eV, respectively.

The global reactivity descriptors calculated using the DFT method play an essential and reliable role to understand the biological activities in many studies. Some of these descriptors are; the global hardness (η), which measures the resistance to change in electron density; chemical potential (μ), measures the escaping tendency of an electron; electronegativity (χ), describes the ability of a molecule to attract electrons towards itself; electrophilicity index (ω), measures the susceptibility of chemical species to accept electrons; softness (S), is the inverse of hardness; the maximum charge transfer (ΔN_{max}), describes the propensity of the system to acquire additional electronic charge from the environment.[27,28] These global reactivity parameters can be defined as:

$$\mu = -\frac{(I+A)}{2} \qquad \chi = -\mu \qquad \eta = \frac{(I-A)}{2} \tag{1}$$

$$\omega = \frac{\mu^2}{2\eta} \qquad S = \frac{1}{2\eta} \qquad \Delta N_{max} = -\frac{\mu}{\eta} \tag{2}$$

where I is the ionization potential ($I = -E_{HOMO}$) and A is the electron affinity ($A = -E_{LUMO}$).

The calculated values of reactivity descriptors of the compounds are listed in Table 3. The hardness (η) values of the compounds are following the order **2f** > **2g** > **2b.** It is expected that the high value of softness (S), defined as the inverse of hardness, is the representative of high reactivity. According to these parameters, **2b** seems the most reactive compound. Also, the E_{gap} of **2b** is the smallest one, this indicates that **2b** is softer than other compounds, its electronic chemical potential (μ) and electrophilicity index *(ω)* values are the greatest and the maximum charge transfer capability (ΔN_{max}) is the highest. The dipole moments of the compounds are 15.136 Debye for **2b**, 7.264 Debye for **2f** and 13.600 Debye for **2g**, proved that the most stable compound is **2f,** while the **2b** is the most reactive.

3. 3. Mulliken Population Analysis, Natural Population Analysis (NPA) and Molecular Electrostatic Potential (MEP)

Mulliken atomic charges and natural population analysis (NPA) play an important role in quantum chemistry. The atomic charge distribution of acceptor and donor atoms in molecules is directly affected by parameters such as polarizability, refractivity, dipole moment, and other electronic structural parameters.[29] Mulliken population charge analysis and natural population analysis of structures were performed using B3LYP/6-31G* level of calculation and a list of all calculated atomic charges are given in Table S1 (see supplementary file). The analyses reveal the presence of electrophilic and nucleophilic atomic charges. According to the results, the bromide anions of the compounds display high nucleophilic behavior with their negative donor atomic charges, while the 2-C-H protons have the highest positive charge value. So, bromide anions attack the hydrogen atom of 2-C carbons, which is the most reactive site of the molecules.

The molecular electrostatic potential (MEP) is related to the electron density and is a useful descriptor in understanding the reactive behavior in both electrophilic and nucleophilic reactions and hydrogen bonding reactions.[30] In the MEP profile, the areas with major positive potential are specified by blue color, which demonstrates the strongest attraction, whereas the maximum negative potential sections have been presented red color, indicates the repulsion. Comparing with the X-ray data it was concluded that the MEP plots proved the intermolecular hydrogen bonds between the bromide anion and cation molecules for all structures (Table 2). The negative potential regions are over the electronegative bromide anions, which are responsible for the intermolecular C–H···Br hydrogen bonds. Also, the N≡C of cyanobenzyl groups of all structures have red colors which means these regions are the electron-rich nucleophilic regions. The net charges of the nitrogen atoms of cyanobenzyl groups confirmed the MEP output.

Table 2. The molecular orbitals for HOMO-LUMO and MEP diagrams of the compounds.

	2b	2f	2g
LUMO +2	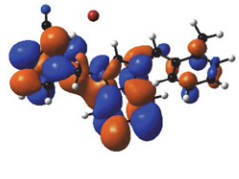	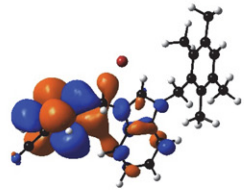	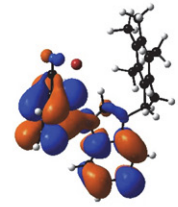
LUMO +1	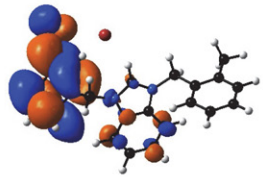	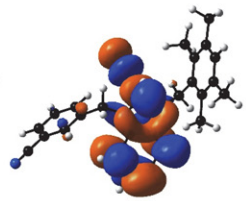	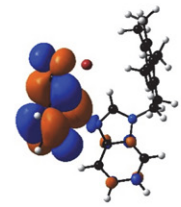
LUMO	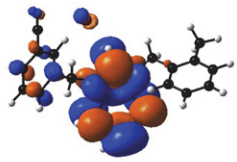	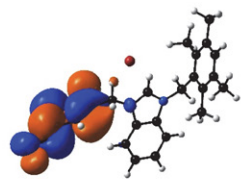	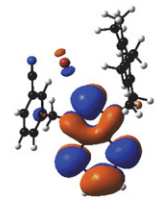
HOMO	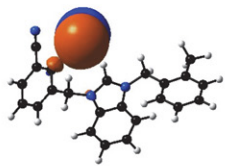	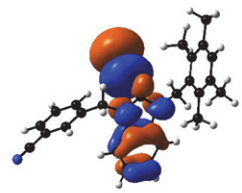	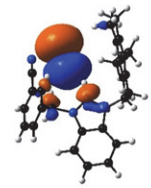
HOMO-1	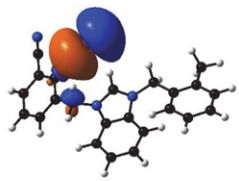	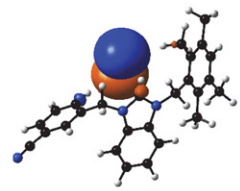	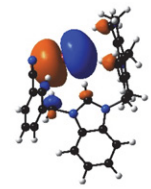
HOMO-2	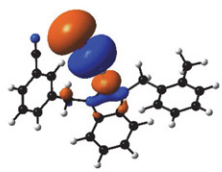	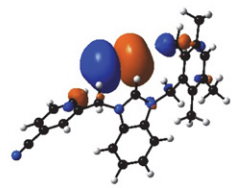	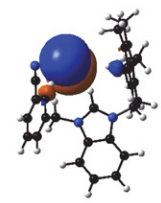
MEP	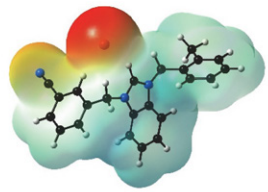	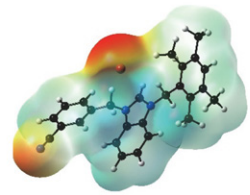	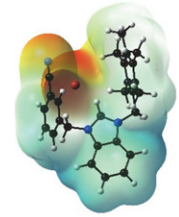

Table 3. Global descriptors of chemical reactivity of *meta*-cyanobenzyl substituted benzimidazolium salts.

(eV)	2b	2f	2g
E_{HOMO} **(-I)**	–4.799	–5.335	–4.861
E_{LUMO} **(-A)**	–1.869	–1.490	–1.850
E_{gap}	2.930	3.845	3.011
Electronegativity χ	3.334	3.413	3.356
Chemical hardness η	1.465	1.923	1.506
Electronic chemical potential μ	–3.334	–3.413	–3.356
Electrophilicity index ω	3.794	3.029	3.739
Softness S	0.341	0.260	0.332
Maximum charge transfer capability ΔN_{max}	2.276	1.775	2.228

3. 4. Natural Bond Orbital (NBO) Analysis

The natural bond orbital analysis (NBO) is an effective method for predicting the stereoelectronic interactions on the reactivity and dynamic behaviors of chemical compounds.[31] It provides a convenient basis for investigating charge transfer or conjugative interaction in molecular systems. The interactions depend on the energy difference between interacting orbitals, and the strong interactions arise between predominant donor and acceptor. The second-order perturbation analysis of the Fock matrix is used to calculate stabilization energy for each donor (i) and acceptor (j) within i→j delocalization. The estimated energy can be determined as $E(2) = \Delta E_{ij} = q_i \frac{F_{i,j}^2}{E_j - E_i}$; where q_i is donor orbital occupancy, E_i and E_j are diagonal elements and F_{ij} is the off-diagonal NBO Fock matrix element. The larger the E(2) value means the more intensive interaction between electron donors and acceptors.[32] The natural bond orbitals' (NBO) calculations for the structures were performed at the DFT/B3LYP/6–31G* method. The stabilization energies of the most important interactions between donor and acceptor along with occupancy are given in Table 4. According to the table, the strongest interactions (π→π*) occur in the NHC ligand for all structures. In the **2b and 2g**, the electron donation from a lone-pair orbital on the carbon atom of benzimidazole, LP(1) C16 and LP(1) C6, to the antibonding acceptors π* N3–C7 (233.49 kJ/mol), π* C12–C14 (58.10 kJ/mol) and π* N3–C4 (219.31 kJ/mol), π* C17–C46 (58.79) orbitals have also high stabilization energies. In the compound **2f**, from the lone-pair orbital of LP(1) N3 to the π* N2–C4 has the energy of 82.11 kJ/mol.

3. 5. UV-Vis Analysis of the Compounds 2b, 2f and 2g

The UV–Vis spectra of the *meta*-cyanobenzyl substituted benzimidazolium salts **2b**, **2f** and **2g** were recorded

Table 4. The Second Order Perturbation Theory Analysis Results of the Fock Matrix in NBO Basis for **2b**, **2f** and **2g** at B3LYP/6-31G* level of the theory.

	Donor(i)	Acceptor(j)	ED_i(e)	ED_j(e)	E(2) kJ/mol	E_j–E_i (a.u)	$F_{i,j}$ (a.u)
2b							
	π* N3–C7	π* N2–C5	0.8166	0.4510	245.94	0.01	0.063
	LP(1) C16	π* N3–C7	1.0440	0.8166	233.49	0.08	0.123
	LP(1) C16	π* C12–C14	1.0440	0.3062	58.10	0.16	0.104
2f							
	π* C6–C9	π* C25–C36	0.4719	0.3343	217.58	0.02	0.082
	π* C10–C11	π* C20–C47	0.3349	0.2821	190.65	0.01	0.081
	π* C6–C9	π* C17–C23	0.4719	0.3274	188.55	0.02	0.082
	π* C19–C45	π* C20–C47	0.3848	0.2821	179.27	0.02	0.082
	LP(1) N3	π* N2–C4	1.5551	0.5650	82.11	0.21	0.122
2g							
	π* N3–C4	π* N2–C9	0.8011	0.4644	321.23	0.01	0.064
	π* C12–C26	π* C8–C33	0.3536	0.3265	261.24	0.01	0.081
	LP(1) C6	π* N3–C4	1.0410	0.8011	219.31	0.08	0.122
	π* C11–C19	π* C8–C33	0.3938	0.3265	177.46	0.02	0.084
	LP(1) C6	π* C17–C46	1.0410	0.3086	58.79	0.16	0.104

with Shimadzu UV-1601 instrument in ethyl alcohol solutions at a concentration of 15 or 20 μM at 25 °C and they were depicted with a range of 200–400 nm. The calculations of the title molecules were performed in ethyl alcohol solvent by using TD-DFT/B3LYP/6-31G* method. Table 5 shows the experimental and calculated UV-Vis spectroscopic parameters (absorption wavelengths (λ), excitation energies and oscillator strengths (*f*). Also, Fig. S2 displays the theoretical UV-Vis spectra of the compounds. The UV–Vis spectra of *meta*-cyanobenzyl substituted benzimidazolium salts **2b**, **2f** and **2g** display four absorption peaks at 220, 230, 250 and 270 nm (Fig. 5). As can be seen in Table 5, the calculated absorption peaks are found to be in close agreement with the experimental ones. The absorption bands between 202 and 288 nm in ethyl alcohol are practically identical and can be attributed to π–π* transitions in the benzene and benzimidazole ring or azomethine (C=N) groups.[33,34] The UV absorbance at an observed excitation wavelength (at 230 and 270 nm) indicates the lowest value for **2b**. These data show that **2b** possesses the lowest molar absorptivity and hence produces the highest quantum yield when compared with **2f** and **2g**.

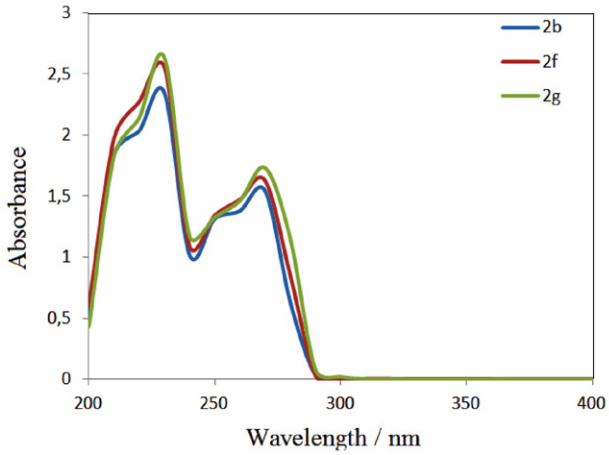

Fig. 5. UV–Vis spectra of the **2b**, **2f** and **2g**

3. 6. Vibrational Analysis

The experimental and calculated FT-IR spectra of the compounds are illustrated in Fig. 6. The unscaled theoretical frequencies using the B3LYP level of theory with 6–31G* basis set along with their IR intensities, probable assignments and potential energy distribution (PED) performed employing VEDA program for all structures are presented in Table S2. As seen in Fig. 6, the experimental fundamentals are nearly consistent with the calculated ones. The probable discrepancies can arise as a result of anharmonic and finite temperature effects.[35] As it is expected that C–H stretching modes belonging to the aromatic ring of the NHC salts were observed and calculated above 3000 cm^{-1}.[36] The 2-C-H stretching modes occur at 2960 cm^{-1} for **2b** and **2f** and 2956 cm^{-1} for **2g**. The calculated assignments are 2772, 3256 and 3025 cm^{-1}, respectively. The benzonitrile N–C stretching vibrations have the

Table 5. The experimental and calculated UV-Vis parameters of the compounds **2b**, **2f** and **2g**.

2b			
Experimental	**The calculated with B3LYP/6-311G(d,p) level in ethyl alcohol**		
λ (nm)	λ (nm)	Excitation energy (eV)	*f* (oscillator strength)
220.00	199.98	6.1999	0.0001
230.00	200.45	6.1853	0.0001
250.00	223.58	5.5454	0.0028
270.00	245.19	5.0566	0.1320
2f			
Experimental	**The calculated with B3LYP/6-311G(d,p) level in gas phase**		
λ (nm)	λ (nm)	Excitation energy (eV)	*f* (oscillator strength)
220.00	201.77	6.1450	0.0208
230.00	203.81	6.0836	0.1032
250.00	221.07	5.6087	0.0046
270.00	232.95	5.3223	0.0015
2g			
Experimental	**The calculated with B3LYP/6-311G(d,p) level in gas phase**		
λ (nm)	λ (nm)	Excitation energy (eV)	*f* (oscillator strength)
220.00	200.45	6.1853	0.0001
230.00	201.06	6.1667	0.0000
250.00	234.01	5.2983	0.0062
270.00	245.19	5.0566	0.1320

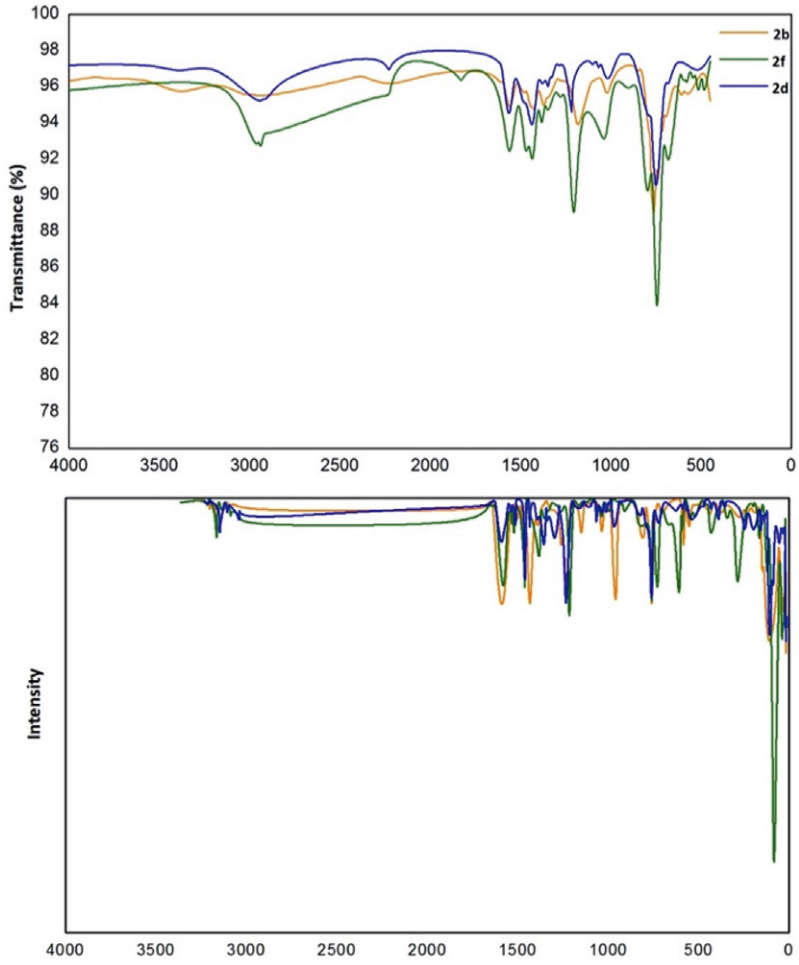

Fig. 6. The experimental (above) and calculated (below) IR spectra of the *meta*-cyanobenzyl substituted benzimidazolium salts.

PED contributions of 89% for all structures; the modes assigned at 2227, 2228 and 2229 cm^{-1}, while they were calculated at 2352, 2348 and 2351 cm^{-1}, respectively.

3. 7. Nuclear Magnetic Resonance (NMR) Studies

The compounds were characterized by ^{1}H, ^{13}C NMR spectroscopy (Figs. S3-8). The theoretical GIAO ^{1}H and ^{13}C chemical shift calculations (with respect to TMS in ppm) were carried out using the DFT/B3LYP method with 6–31G* basis set and compared with experimental chemical shift values (Tables S3, S4). The chemical shifts are converted to the TMS scale by subtracting the calculated absolute chemical shielding of TMS ($\delta = \Sigma_0 - \Sigma$) where δ is the chemical shift, Σ is the absolute shielding and Σ_0 is the absolute shielding of TMS, whose values are 32.18 and 189.73 ppm for B3LYP/6-31G*, respectively. There are some deviations of the chemical shift values, which may be due to the chemical environment of the C and H atoms in the molecules.

According to the tables, the signals of the 2-C carbons appeared at 143.55, 142.2 and 134.4 ppm, while they were calculated at 139.27, 127.10 and 124.52 ppm, respectively. Hydrogen bonding has been recognized as the main interaction between the cations and anions of azolium salts leading to close arrangement between the counter anions and the most acidic 2-C–H proton.[37–40] A strong hydrogen bond acceptor is expected to polarize the 2-C–H bond and slightly increase the acidity of the salt. As anticipated, bromide anions with four lone pairs of electrons are the hydrogen bonding acceptors that lead to the most downfield shifts of the ^{1}H NMR for 2-C–H signal. These hydrogen bonding interactions were also determined by single-crystal X-ray diffraction studies.[10] The most acidic protons (2-C–H) were observed at 10.13, 9.42 and 9.34 ppm, and calculated at 16.14, 9.81 and 12.79 ppm, respectively. The data also showed that the methylene carbon atoms had the least chemical shift values.

3. 8. Computer-Aided Prediction of Biological Activities of the *Meta*-cyanobenzyl-substituted Benzimidazolium Salts

The PASS (Prediction of Activity Spectra for Substances) computer program is an estimation tool, which allows predicting the probable profile of biological activity of a

Table 6. Biological activity assessment using PASS online software.

Activity	2b		2f		2g	
	P_a	P_i	P_a	P_i	P_a	P_i
Analgesic	0.885	0.004	0.854	0.005	0.874	0.004
Substance P antagonist	0.880	0.002	0.859	0.002	0.880	0.002
Analgesic, non-opioid	0.843	0.004	0.805	0.005	0.827	0.005
Antiinflammatory	0.769	0.009	0.787	0.008	0.751	0.010
CYP2H substrate	0.653	0.049	0.633	0.055	0.653	0.049
CYP2C19 inducer	0.557	0.008	0.546	0.008	0.557	0.008
Acetylcholine neuromuscular blocking agent	0.557	0.041	0.529	0.057	0.557	0.041

drug-like organic compound based on its structural formula. The average accuracy of prediction is about 95% according to leave-one-out-cross validation (LOOCV) estimation.[41,42]

The biological activity spectra of the *meta*-cyanobenzyl substituted benzimidazolium salts were theoretically obtained by the PASS Online program and the analysis results were enlisted in Table 6. According to the data, all compounds are very likely to be analgesic, Substance P antagonist, non-opoid analgesic and anti-inflammatory with corresponding P_a values, which are higher than 0.7. Compounds also exhibit activity to the CYP2H substrate and CYP2C19 inducer. In our previous study, potential AChE inhibition properties of the compounds were investigated.[10] PASS online studies proved that these compounds can be used as acetylcholine neuromuscular blocking agents, as well.

4. Conclusion

As a result, this study contains theoretical aspects of three *meta*-cyanobenzyl substituted NHC precursors. The biological reactivity of the compounds was predicted by global reactivity descriptors and using PASS (prediction of activity spectra for biologically active structures) online. DFT and PASS online studies pointed out the activation of the compounds. The compound **2b** was found to be the most reactive structure by both computational methods. These results were found to be compatible with the experimental biological activity studies. The molecular and crystal structure of **2b** was also determined by using the single-crystal X-ray diffraction method. Natural bond orbital (NBO) analysis was used to analyze the stability of the molecules arising from hyperconjugative interactions and charge delocalization. The vibrational frequencies, chemical shifts and absorption wavelengths were calculated and compared to the experimental ones. Biological activity predictions showed that all structures have a high analgesic, substance P antagonist and non-opoid analgesic activities.

Supplementary

Crystallographic data as .cif files for the structure reported in this paper have been deposited at the Cambridge Crystallographic Data Center with CCDC 1971777 for **2b**. Copies of the data can be obtained free of charge at http://www.ccdc.cam.ac.uk/conts/retrieving.html or from the Cambridge Crystallographic Data Center, 12, Union Road, Cambridge CB2 1EZ, UK. Fax: (+44) 1223-336-033, email: deposit@ccdc.cam.ac.uk.

Acknowledgments

The authors acknowledge İnönü University Scientific and Technology Center for the spectroscopic data and Dokuz Eylül University for the use of the Oxford Rigaku Xcalibur Eos Diffractometer (purchased under University Research Grant No: 2010.KB.FEN.13). The authors also thank Assoc. Prof. Dr. Muhittin Aygün for the use of the Gaussian 09W/Gauss View package program.

5. References

1. S. Diez-Gonzalez, N. Marion, S. P. Nolan, *Chem. Rev.* **2009**, *109*, 3612–3676. **DOI:**10.1021/cr900074m
2. H. W. Wanzlick, H. J. Schönherr, Angew. Chem. Int. Ed. Engl. **1968**, *7*, 141–142. **DOI:**10.1002/anie.196801412
3. K. Öfele, J. Organomet. Chem. **1968**, *12*, 42–43. **DOI:**10.1016/S0022-328X(00)88691-X
4. A. J. III Arduengo, R. L. Harlow, M. Kline, J. Am. Chem. Soc. **1991**, *113*, 361–363. **DOI:**10.1021/ja00001a054
5. S. Akkoç, V. Kayser, I. Ö. İlhan, D. E. Hibbs, Y. Gök, P. A. Williams, B. Hawkins, F. Lai, *J. Organomet. Chem.* **2017**, *839*, 98–107. **DOI:**10.1016/j.jorganchem.2017.03.037
6. I. Yıldırım, A. Aktaş, D. Barut Celepci, S. Kırbağ, T. Kutlu, Y. Gök, M. Aygün, *Res. Chem. Intermed.* **2017**, *43*, 6379–6393. **DOI:**10.1007/s11164-017-2995-3
7. Y. Gök, S. Akkoç, H. Erdoğan, S. Albayrak, *J. Enzyme Inhib. Med. Chem.* **2016**, *31*, 1322–1327. **DOI:**10.3109/14756366.2015.1132210
8. S. Budagumpi, S. Endud, *Organometallics* **2013**, *32*, 1537–1562. **DOI:**10.1021/om301091p
9. Y. Sarı, A. Aktaş, P. Taslimi, Y. Gök, İ. Gülçin, *J. Biochem. Mol. Toxicol.* **2018**, *32*, e22009. **DOI:**10.1002/jbt.22009
10. F. Türker, D. Barut Celepci, A. Aktaş, P. Taslimi, Y. Gök,

M. Aygün, İ. Gülçin, *Arch Pharm Chem Life Sci.* **2018,** *351*, e1800029. **DOI:**10.1002/ardp.201800029
11. P. K. Chattaraj, S. Nath, and B. Maiti, Computational Medicinal Chemistry for Drug Discovery, **2003**, Marcel Dekker, New York.
12. CrysAlis^{Pro} Software System, Version 1.171.38.43, **2015**, Rigaku Corporation, Oxford, UK.
13. R. C. Clark, J. S. Reid, *Acta Crystallogr. A*. **1995**, *51*, 887–897. **DOI:**10.1107/S0108767395007367
14. G. M. Sheldrick, *Acta Crystallogr. A*. **2015**, *71*, 3–8. **DOI:**10.1107/S2053273314026370
15. G. M. Sheldrick, *Acta Crystallogr. C.* **2015**, *71*, 3–8. **DOI:**10.1107/S2053273314026370
16. O. V. Dolomanov, L. J. Bourhis, R. J. Gildea, J. A. K. Howard, H. Puschmann, *J. Appl. Cryst.* **2009**, *42*, 339–341. **DOI:**10.1107/S0021889808042726
17. M. J. Frisch, G. W. Trucks, H. B. Schlegel, G. E. Scuseria, M. A. Robb, J. R. Cheeseman, G. Scalmani, V. Barone, G. A. Petersson, H. Nakatsuji, X. Li, M. Caricato, A. Marenich, J. Bloino, B. G. Janesko, R. Gomperts, B. Mennucci, H. P. Hratchian, J. V. Ortiz, A. F. Izmaylov, J. L. Sonnenberg, D. Williams-Young, F. Ding, F. Lipparini, F. Egidi, J. Goings, B. Peng, A. Petrone, T. Henderson, D. Ranasinghe, V. G. Zakrzewski, J. Gao, N. Rega, G. Zheng, W. Liang, M. Hada, M. Ehara, K. Toyota, R. Fukuda, J. Hasegawa, M. Ishida, T. Nakajima, Y. Honda, O. Kitao, H. Nakai, T. Vreven, K. Throssell, J. A. Montgomery, Jr., J. E. Peralta, F. Ogliaro, M. Bearpark, J. J. Heyd, E. Brothers, K. N. Kudin, V. N. Staroverov, T. Keith, R. Kobayashi, J. Normand, K. Raghavachari, A. Rendell, J. C. Burant, S. S. Iyengar, J. Tomasi, M. Cossi, J. M. Millam, M. Klene, C. Adamo, R. Cammi, J. W. Ochterski, R. L. Martin, K. Morokuma, O. Farkas, J. B. Foresman, and D. J. Fox, Gaussian 09, Revision D.01. **2013**, Gaussian, Inc., Wallingford CT.
18. R. Dennington, T. A. Keith, J.M. Millam, GaussView, Version 6, **2016**, Semichem Inc., Shawnee Mission, KS.
19. E.D. Glendening, J.K. Badenhoop, A.E. Reed, J.E. Carpenter, F. Weinhold, NBO Version 3.1. **1995**, Theoretical Chemistry Institute, University of Wisconsin, Maddison.
20. M. H. Jamroz, Vibrational Energy Distribution Analysis VEDA 4. **2004–2010**, Warsaw.
21. R. Ditchfield. *J. Chem. Phys.* **1972***, 56*, 5688–5691. **DOI:**10.1063/1.1677088
22. S. Gunasekaran, R. A. Balaji, S. Kumeresan, G. Anand, S. Srinivasan, *Can. J. Anal. Sci. Spectrosc.* **2008**, *53*, 149–162.
23. J. Fleming, Frontier Orbitals and Organic Chemical Reactions. **1976**, John Wiley & Sons, New York.
24. V. Arjunan, L. Devi, R. Subbalakshmi, T. Rani, S. Mohan, *Spectrochim. Acta A*. **2014**, *130*, 164–177. **DOI:**10.1016/j.saa.2014.03.121
25. O. A. El-Gammal, T. H. Rakha, H. M. Metwally, G. M. Abu El-Reash, *Spectrochim. Acta A*. **2014**, *127*, 144–156. **DOI:**10.1016/j.saa.2014.02.008
26. R. Bahnasawy, E. Shereafy, T. Kashar, *J. Thermal Anal. Calorimetry,* **1993**, *39*, 65–74. **DOI:**10.1007/BF02235447
27. H. Chermette, *J. Comput. Chem.* **1999**, *20*, 129–154. **DOI:**10.1002/(SICI)1096-987X(19990115)20:1<129::AID-JCC13>3.0.CO;2-A
28. L. H. Mendoza-Huizar, *Acta Chim. Slov.* **2014**, *61*, 694–702.
29. R. S. Mulliken, *J Chem. Phys*. **1955**, *23*, 1833–1840. **DOI:**10.1063/1.1740588
30. N. Okulik, A. H. Jubert, *Internet Electron. J. Mol. Des.* **2005**, *4*, 17–21.
31. P. Singh, S.S. Islam, H. Ahmad, A. Prabaharan, *J Mol. Struct.* **2018**, *1154*, 39–50. **DOI:**10.1016/j.molstruc.2017.10.012
32. R. J. Xavier, E. Gobinath, *Spectrochim Acta A*. **2012**, *86*, 242–251. **DOI:**10.1016/j.saa.2011.10.031
33. A. Kılıç, E. Tas, İ. Yılmaz, *J Chem. Sci.* **2009**, *121*, 43–56. **DOI:**10.1007/s12039-009-0005-z
34. A. Aktas¸ D. Barut Celepci, Y. Gök. *J Chin Chem Soc.* **2019**, *66*, 1389–1396. **DOI:**10.1002/jccs.201900020
35. M. Katari, E. Nicol, V. Steinmetz, G. van der Rest, D. Carmichael, G. Frison. *Chem. Eur. J*. **2017**, *23*, 8414–8423. **DOI:**10.1002/chem.201700340
36. S. Gunasekaran, S. Ponnusamy. *Indian J. Pure Ap. Phy.* **2005**, *43*, 838–843.
37. A. G. Avent, P. A. Chaloner, M. P. Day, K. R. Seddon, T. Welton, *J. Chem. Soc. Dalton Trans*. **1994**, *23*, 3405–3413. **DOI:**10.1039/dt9940003405
38. J. A. Cowan, J. A. C. Clyburne, M. G. Davidson, R. L. W. Harris, J. A. K. Howard, P. Kupper, M. A. Leech, S. P. Richards, *Angew. Chem. Int. Ed.* **2002**, *41*, 1432–1434. **DOI:**10.1002/1521-3773(20020415)41:8<1432::AID-ANIE1432>3.0.CO;2-M
39. N. Kuhn, A. Alsheikh, *Coord. Chem. Rev.* **2005**, *249*, 829–857. **DOI:**10.1016/j.ccr.2004.10.003
40. H. V. Huynh, T. T. Lam, H. T. T. Luong, *RSC Adv.* **2018**, *8*, 34960–34966. **DOI:**10.1039/C8RA05839C
41. D. A. Filimonov, A. A. Lagunin, T. A. Gloriozova, A. V. Rudik, D. S. Druzhilovskii, P. V. Pogodin, V. V. Poroikov, *Chem Heterocyc Compd*. **2014**, *50*, 444–457. **DOI:**10.1007/s10593-014-1496-1
42. D. A. Filimonov, V. V. Poroikov, *RSC Publishing*, **2008**, Cambridge, 182–216.

Povzetek

Teoretično smo preučevali strukturne lastnosti prekurzorjev *N*-heterocikličnih karbenov (NHC), ki so bili substituirani z meta-cianobenzilom. Molekularno in kristalno strukturo ene od spojin smo določili z rentgensko difrakcijsko metodo. Deskriptorje globalne reaktivnosti smo analizirali z metodo gostotnega funkcionala (DFT) B3LYP z baznim setom 6-31G *, da bi razumeli biološko aktivnost spojin. Izračunali smo vibracijske frekvence, kemične premike in absorpcijske valovne dolžine in jih primerjali z eksperimentalnimi podatki. Napovedovalna študija biološke aktivnosti je bila narejena s pomočjo spletne programske opreme PASS (= prediction of activity spectra for biologically active structures) in je pokazala, da imajo spojine analgetično, antagonistično (na snov P), neopioidno in protivnetno aktivnost.

Except when otherwise noted, articles in this journal are published under the terms and conditions of the Creative Commons Attribution 4.0 International License